

# The merit of the North Sea-Caspian pattern in explaining climate variability in the Euro-Mediterranean region

Ferat Çağlar<sup>1</sup>  | Omer Yetemen<sup>1</sup>  | Kwok Pan Chun<sup>2</sup>  | Omer Lutfi Sen<sup>1</sup> 

<sup>1</sup>Eurasia Institute of Earth Sciences,  
Istanbul Technical University, Istanbul,  
Turkey

<sup>2</sup>Department of Geography and  
Environmental Management, University  
of the West of England, Bristol, UK

## Correspondence

Ferat Çağlar, Eurasia Institute of Earth  
Sciences, Istanbul Technical University,  
34469 Maslak, Istanbul, Turkey.  
Email: [caglarf@itu.edu.tr](mailto:caglarf@itu.edu.tr)

## Funding information

Türkiye Bilimsel ve Teknolojik Arastırma  
Kurumu, Grant/Award Number: 118C329

## Abstract

Teleconnection patterns are one of the key features to understanding high-frequency natural climate variability. The North Sea-Caspian Pattern (NCP) was identified as a middle tropospheric dipole and its hydroclimatological implications have been substantially restricted to the Eastern Mediterranean region. Thus, the hydroclimatological influences of the NCP in the Euro-Mediterranean region were investigated via a comparative approach with dominant tropospheric teleconnections in the Eurasian region and synoptic features such as ridge-trough positioning and strength. By using high-resolution ERA5 reanalysis data, cross-correlations between indexes, anticorrelations at 500 hPa and composite anomaly maps for seasonally representative months were produced to understand the working mechanism of the NCP. Comparisons included the East Atlantic/Western Russian (EAWR) pattern, a rotated principal component analysis (RPCA) variant of NCP which utilizes pole-based representation. Analysis revealed that the NCP was correlated well with the Mediterranean trough displacement and with the strength of the East Asian trough. Climate anomalies indicated by the NCP were greater and more spatially consistent compared to other teleconnections. The NCP also showed higher contrasts of temperature and precipitation than the EAWR based on the composite anomaly maps. In conclusion, the NCP explained climate variability in all seasons linking remote centres of action within Eurasia's east and west extremes.

## KEYWORDS

AO, EAWR, Euro-Mediterranean, hydro-climatology, Mediterranean trough, NAO, NCP, teleconnections

## 1 | INTRODUCTION

Climate variability is often investigated through teleconnections, also referred to as preferred modes of variability (Ångström, 1935; Panagiotopoulos et al., 2002). Teleconnection patterns are commonly identified through the correlation method and Rotated Principle Component

Analysis (RPCA) (Hatzaki et al., 2007; Nigam & Baxter, 2015). The correlation method is more straightforward but involves a subjective routine of choosing the poles of teleconnections, whereas the RPCA method is more systematic. It does, however, also involve processes that might affect the results of analyses, such as defining the domain where eigenvectors are calculated.

This is an open access article under the terms of the [Creative Commons Attribution](https://creativecommons.org/licenses/by/4.0/) License, which permits use, distribution and reproduction in any medium, provided the original work is properly cited.

© 2023 The Authors. *International Journal of Climatology* published by John Wiley & Sons Ltd on behalf of Royal Meteorological Society.

Barnston and Livezey (1987) studied the lower troposphere using the RPCA method to identify many of the teleconnections frequently utilized in the Northern Hemisphere, and demonstrated that the North Atlantic Oscillation (NAO) is the most prominent one. The NAO is a north–south pressure dipole located at the upstream of the Euro-Mediterranean (EM) region (Hurrell et al., 2003). It is observable yearlong and is asserted to control most of the teleconnection patterns in the Northern Hemisphere (Barnston & Livezey, 1987). These characteristics of the NAO have stimulated remarkable attention. However, the NAO was not defined as the most representative index in terms of hydro-meteorological variability, specifically outside of winter (Ionita, 2014; Ionita et al., 2020; Zhu et al., 2017). When principal component analysis (PCA) is applied to sea level pressure (SLP) data instead of 700 hPa, the Arctic Oscillation (AO) pattern becomes the leading mode (Thompson & Wallace, 1998). The AO is an annular mode, which is roughly a superimposed pattern on the NAO that has an extra pole over the Pacific (Ambaum et al., 2001). Other useful teleconnections for indicating low-frequency changes in the EM region are listed as the East Atlantic (EA), the East Atlantic/Western Russia (EAWR), the Polar/Eurasia (POLEUR), the Scandinavian (SCAN), the Atlantic Multidecadal Oscillation (AMO) (Gao et al., 2017), the Mediterranean Oscillation (MO) (Criado-Aldeanueva & Soto-Navarro, 2020), and the North Sea-Caspian Pattern (NCP) (Kutiel & Benaroch, 2002).

The EAWR pattern, also referred to as the Eurasian (Esbensen, 1984; Wallace & Gutzler, 1981) or Eurasian-2 pattern (Barnston & Livezey, 1987) in the earlier literature, was introduced as a tricentric lower troposphere (700 hPa) teleconnection, identified by using RPCA. The poles of the EAWR pattern are located between the UK and Denmark, north of the Caspian Sea, and north of Korea, where the pole at the Caspian Sea has an opposite sign (Barnston & Livezey, 1987). Two poles of the NCP proximate to two of the EAWR, which are positioned in the west. The similarity between these two teleconnection patterns was already mentioned in the study that identified the NCP (Kutiel & Benaroch, 2002); however, neither the correlation between the time series of the EAWR and the NCP patterns nor their indication of anomalies in atmospheric fields has been explored thoroughly.

The interaction occurring between the East Atlantic and West Pacific was characterized through eastward propagating Rossby wave trains (Cheung et al., 2012; Gao et al., 2017; Li et al., 2008; Lim, 2015). The North Sea is a usual location for blocking events that limit moisture advection into Europe and alter storm tracks (Lionello

et al., 2006). The Ural-Siberian region is another location of frequent blocking events, with effects reaching the west coast of the Pacific (He et al., 2017). The Ural blocking pattern observed in winter also forms due to eastward propagating Rossby wave trains, and they have been found to be significantly correlated with the AO (Cheung et al., 2012). A strong connection between the strength of the East Asian Trough (EAT) located in the western Pacific and the east–west displacement of the Mediterranean Trough (MedT) have been shown to cause variations in temperature and precipitation patterns over the EM region in winter (Sen et al., 2019). The location chosen to depict the strength of the EAT overlaps with the eastern pole (north of Korea) of the EAWR pattern, and the MedT displacement occurs somewhere between the edges of Europe, that are somewhat represented by the poles of both the EAWR pattern and the NCP. Displacement of ridge-trough patterns in a region can significantly control climate variability, particularly in the cold season (Xoplaki et al., 2004).

Previous NCP studies have investigated its climate implications in Greece, Turkey, Iran and Israel by utilizing weather station data (Ghasemi & Khalili, 2008; Kutiel, 2011; Kutiel et al., 2002; Kutiel & Benaroch, 2002; Kutiel & Türkeş, 2005; Tatli, 2007; Unal et al., 2012). One study utilizing ERA40 re-analysis data revealed that the NCP explains precipitation fluxes in Central and Western Europe (Gündüz & Özsoy, 2005). Although a strong connection was detected between the NCP and temperature anomalies, the influence on precipitation was found to be relatively weak in the Eastern Mediterranean and Asia Minor regions. Therefore, subsequent NCP studies did not investigate beyond these regions. Only recent studies suggested that the NCP could be a good indicator of precipitation in the EM region, specifically in central and northwest Europe (Çağlar et al., 2021; He et al., 2022; Müller-Plath et al., 2022). Even though the influence of the NCP on precipitation has been neglected in a broader region, its related pattern, the EAWR, was found to be a good indicator of precipitation anomalies in Europe, the Balkan Peninsula and the Scandinavian region in winter (Ionita, 2014; Krichak et al., 2002). Teleconnections research, including research on the EM region, largely focuses on the cold season, which has the highest precipitation and greatest variability in atmospheric fields (Esbensen, 1984; Hurrell, 1995; Ionita, 2014; Krichak et al., 2002; Krichak & Alpert, 2005a, 2005b; Krown, 1966; Kutiel et al., 2002; Panagiotopoulos et al., 2002; Sen et al., 2019; Wallace & Gutzler, 1981; Xoplaki et al., 2004).

The present study aimed to investigate the capability of the NCP in explaining climate variability in the EM region compared with other teleconnection patterns and

synoptic features influencing the region. Besides investigations on limited geographical scope, understanding regarding working mechanism of NCP is scarce. Therefore, we aimed to examine the working mechanism of the NCP and provide descriptions for its interactions, impacts, and borders. We also evaluated different representations of the NCP and EAWR pattern to understand which one would be more suitable to indicate climate variability more distinctively.

## 2 | DATA AND METHOD

Except for those readily available in the Climate Prediction Center (CPC), indexes of interest were calculated using the European Center for Medium-Range Forecast (ECMWF) ERA5 re-analysis data. Monthly 2-meter temperature, precipitation, and 500 hPa geopotential height from the same data set were used for the assessment of climate variability. ERA5 replaces the ERA-Interim re-analysis project, improving the horizontal resolution from 80 to 31 km. It is available for download on  $0.25^\circ \times 0.25^\circ$  grids and covers the entire period from 1950 to the present (Bell et al., 2021; Hersbach et al., 2020). Our research area (EM) is bounded by  $20^\circ\text{W}$ – $60^\circ\text{E}$  longitudes, and  $25^\circ$ – $75^\circ\text{N}$  latitudes that cover Europe, western Asia, the Mediterranean Sea and North Africa.

The NCP index makes use of the standardized monthly mean 500 hPa height differences between the North Sea ( $0^\circ$ – $10^\circ\text{E}$ ,  $55^\circ\text{N}$ ) and Caspian ( $50^\circ$ – $60^\circ\text{E}$ ,  $45^\circ\text{N}$ ) to indicate climate anomalies (Kutiel & Benaroch, 2002). To understand the working mechanism of the NCP and the way it represents Euro-Mediterranean climate deviations, we calculated the trough displacement index (TDI) (Sen et al., 2019), which is an attempt to digitize the east-west displacement of Mediterranean Trough (TDI\_MedT) by  $z_{500}$  height differences between the points located at  $39^\circ\text{N}$ ,  $10^\circ\text{E}$  and  $39^\circ\text{N}$ ,  $50^\circ\text{E}$ . We also calculated the trough intensity indexes (TII) using  $z_{500}$  mean thickness between  $20^\circ$ – $45^\circ\text{E}$  and  $30^\circ$ – $50^\circ\text{N}$  for MedT (TII\_MedT) and between  $125^\circ$ – $145^\circ\text{E}$  and  $30^\circ$ – $45^\circ\text{N}$  for East Asian Trough (TII\_EAT) (Sen et al., 2019). All of the indices were calculated by using averages and standard deviations from 1981 to 2010 for each month to compare the NCP index with other available indexes. MO was assessed using various methods: representations calculated using stations located at the west and east sides of the Mediterranean, and the PCA of SLP (Criado-Aldeanueva & Soto-Navarro, 2013, 2020). We utilized the original definition of MO that uses 500 hPa anomalies between Algiers and Cairo (Conte et al., 1989).

The monthly teleconnection indices of the AO, the NAO and the EAWR pattern were obtained from the

CPC (<https://www.cpc.ncep.noaa.gov>). The CPC utilizes the RPCA method described by Barnston and Livezey (1987) to calculate teleconnection indexes; instead of 700 hPa, the CPC uses 500 hPa field of NCEP-NCAR re-analysis (Kalnay et al., 1996; Kistler et al., 2001) in the Northern Hemisphere ( $20^\circ$ – $90^\circ\text{N}$ ) (Climate Prediction Center Internet Team, 2008). The CPC also provides standardized climate indexes using averages and standard deviations of the 1981–2010 period.

The correlation coefficients of  $z_{500}$  height were calculated to investigate the location and strength of dependency between these centres of action with the associated teleconnection indices. This analysis covered a larger domain to include interactions occurring on the suspected full extent of the NCP, for example, interactions occurring at the Pacific coast of Asia, which were digitized via TII\_EAT.

It should be noted that not all teleconnection indexes in this study were calculated using the same re-analysis data, which can cause differences in index values. To assess data sensitivity, we calculated the NCP using both NCEP-NCAR and ERA5 re-analysis data. The Pearson correlation coefficient between these two NCP indexes was  $r = 0.996$ , and the coefficient of determination was  $R^2 = 0.992$ , which indicated that using different data sources had a negligible effect on results. The agreement between two versions of the NCP dramatically increases after 1975, which is the start of the satellite era (not shown).

We also applied the Kolmogorov–Smirnov (KS) test for temperature and precipitation data grouped by phases. KS is a nonparametric test to check whether the distributions of two samples are significantly different. We chose a nonparametric test because the distributions of parameters were location specific, and we were working on a broad region. Differences between positive (+) and negative (–) years were tested. We carried out a composite analysis of  $z_{500}$  height, temperature and precipitation fields according to standardized scores of teleconnection indexes. Standardized scores  $z_i$  were classified into three groups;  $z_i \geq 0.5$  were regarded as positive (+),  $z_i \leq -0.5$  as negative (–) and  $z_i < |0.5|$  as neutral (N).

We used National Center for Atmospheric Research (NCAR) Command Language (NCL) software for composite analysis and mapping, as well as the `kolsm2_n` function for the KS test (The NCAR Command Language, 2019). Pearson cross-correlation matrices of monthly climate indexes, seasonal subsets of monthly climate indexes, and their statistical significance levels were calculated using the R software `ggpairs` package (Schloerke et al., 2021) (i.e., December, January and February cross-correlations were calculated through time steps 1950-12, 1951-01, 1951-02, 1951-12, ..., 2018-12,

TDI_MedT	MO	TII_EAT	CPC_EAWR	CPC_AO	CPC_NAO	
Corr: 0.380*** DJF: 0.595*** MAM: 0.476*** JJA: -0.016 SON: 0.406***	Corr: 0.121*** DJF: 0.321*** MAM: 0.155* JJA: -0.143* SON: 0.098	Corr: 0.139*** DJF: 0.318*** MAM: 0.064 JJA: -0.034 SON: 0.183**	Corr: 0.488*** DJF: 0.809*** MAM: 0.356*** JJA: 0.288*** SON: 0.536***	Corr: 0.315*** DJF: 0.390*** MAM: 0.264*** JJA: 0.303*** SON: 0.310***	Corr: 0.360*** DJF: 0.124. MAM: 0.307*** JJA: 0.494*** SON: 0.491***	NCP
	Corr: 0.723*** DJF: 0.784*** MAM: 0.709*** JJA: 0.644*** SON: 0.747***	Corr: 0.172*** DJF: 0.429*** MAM: 0.046 JJA: -0.026 SON: 0.223**	Corr: 0.278*** DJF: 0.591*** MAM: 0.148* JJA: 0.172* SON: 0.248***	Corr: 0.254*** DJF: 0.489*** MAM: 0.324*** JJA: -0.111 SON: 0.318***	Corr: 0.180*** DJF: 0.361*** MAM: 0.318*** JJA: -0.130. SON: 0.159*	TDI_MedT
		Corr: 0.111** DJF: 0.308*** MAM: -0.047 JJA: 0.069 SON: 0.085	Corr: 0.185*** DJF: 0.451*** MAM: 0.027 JJA: 0.123. SON: 0.169*	Corr: 0.199*** DJF: 0.371*** MAM: 0.240*** JJA: -0.029 SON: 0.211**	Corr: 0.097** DJF: 0.343*** MAM: 0.214** JJA: -0.158* SON: -0.052	MO
			Corr: 0.063. DJF: 0.358*** MAM: 0.093 JJA: -0.119. SON: -0.048	Corr: 0.307*** DJF: 0.466*** MAM: 0.256*** JJA: 0.269*** SON: 0.237***	Corr: 0.120*** DJF: 0.245*** MAM: 0.061 JJA: 0.008 SON: 0.164*	TII_EAT
				Corr: 0.041 DJF: 0.295*** MAM: 0.044 JJA: -0.175* SON: 0.068	Corr: 0.045 DJF: 0.081 MAM: -0.018 JJA: 0.020 SON: 0.073	CPC_EAWR
					Corr: 0.640*** DJF: 0.746*** MAM: 0.614*** JJA: 0.652*** SON: 0.560***	CPC_AO

**FIGURE 1** Pearson cross-correlations between the standardized monthly teleconnection indices and the monthly correlations of the seasonal subsets. Corr, Correlation; DJF, December–February; JJA, June–August; MAM, March–May; SON, September–November; NCP, North Sea-Caspian pattern; TDI\_MedT, Mediterranean Trough Displacement Index; MO, Mediterranean Oscillation; TII\_EAT, Mediterranean Trough Intensity Index; CPC, Climate Prediction Center; CPC\_EAWR, East Atlantic/Western Russian Index obtained from CPC; CPC\_AO, Arctic Oscillation Index obtained from CPC; CPC\_NAO, North Atlantic Oscillation Index obtained from CPC [Colour figure can be viewed at [wileyonlinelibrary.com](http://wileyonlinelibrary.com)]

2019-01, 2019-02, 2019-12). Hereafter, seasons are abbreviated as followed: DJF—December, January, February; MAM—March, April, May; JJA—June, July, August; SON—September, October, November.

Teleconnections are often described as opposite signed anomalies in pressure fields. To capture that

feature, Kutiel and Benaroch (2002) utilized an anticorrelation analysis on a coarser resolution gridded reanalysis data. Similarly, we re-gridded ERA5 data to an N9 resolution Gaussian grid using first order conservative mapping via Climate Data Operators (CDO) (Schulzweida, 2022). Grid points with statistically

significant ( $p < 0.05$ ) negative correlations based on NCL's rtest were then connected with lines (The NCAR Command Language, 2019). Results were plotted with Arc Pro 2.9 software using graduated symbols and graduated colour visualization methods based on correlation coefficients.

### 3 | RESULTS AND DISCUSSION

#### 3.1 | Cross-correlations between indexes

A cross-correlation analysis was conducted to investigate to what extent the NCP was related to other chosen indexes in the region. Results of the monthly and seasonal subsets of monthly correlations were given in Figure 1. The NCP had the highest correlation coefficients with the EAWR pattern for monthly and seasonal subsets, which indicates that these teleconnections are similar. The NCP and TDI\_MedT were significantly correlated when scores were highest, in winter, decreasing in MAM and SON, and uncorrelated in JJA. The EAWR pattern was also significantly correlated with TDI\_MedT. Although overall scores were lower compared to the NCP-TDI\_MedT scores, the EAWR had weak but significant correlations with TDI\_MedT in JJA. The relationship between NCP or TDI\_MedT and TII\_EAT was moderate and significant in the cold half of the year.

The east to west shift of hydroclimatological variables in the EM was also attributed to MO in the earlier studies. Correlations between NCP and MO were weaker than those between NCP and TDI\_MedT, but still statistically significant. This suggests that the NCP was more strongly coupled to trough positioning within EM rather than MO. The MO-TDI\_MedT relationship was strongest among all others and consistent in all seasons, which suggests that while studying longitudinal oscillations within the EM, the role of TDI\_MedT should be closely investigated.

The NCP-AO relationship was statistically significant for all seasons with the highest  $r$  value for winter. This was where the NCP and EAWR pattern differ the most, since the EAWR pattern was only correlated with the AO in DJF. Therefore, we can conclude that as the NCP was more sensitive to the AO, it has also been affected by the number and amplitude of Rossby waves.

For most of the cross-correlations examined, the observed relationships get weaker in transition seasons and become the weakest in summer. Decay in correlation might be attributed to the northward shift and weakening of the Mediterranean trough. In summer, the Hadley cell in the Northern Hemisphere shifts northward, and

the high-pressure zone under the descending branch causes increased blocking occurrences and less trough formations in the Mediterranean. Using fixed geographical poles for dynamical features with seasonal spatial deviation might have caused misrepresentations. In some cases, it is uncertain whether the relationship is absent, or if the index fails to represent the process.

Poles of TDI\_MedT were chosen to represent a migration in the east-west direction specifically in winter (Sen et al., 2019). To examine this further, the first three EOFs were calculated by using the seasonal mean  $Z_{500}$  of DJF for the region  $25^{\circ}$ – $55^{\circ}$ N,  $0^{\circ}$ – $60^{\circ}$ E. The percentages of the explained variations were found to be 38.2%, 26.5% and 12.7% in EOF1, EOF2 and EOF3, respectively (Figure S1, Supporting Information). The loading patterns (eigenvectors) were in agreement with those in Sen et al. (2019). As the EOF1 loading pattern was interpreted as an indicator of trough displacement, the correlation of PC1 of MedT time series (PC1\_MedT) with the NCP was checked to see whether the NCP has any capability to indicate the Mediterranean Trough migration. The correlation was  $-0.877$  (it should be noted sign is arbitrary in EOF analysis) for NCP, which was as good as that found between PC1\_MedT and TDI\_MedT ( $-0.867$ ; the cross-correlation results of NCP, TDI\_MedT and the first three PC's are given in Figure S2). This demonstrates further evidence that the NCP is a good indicator of the trough displacement in the east-west direction during the winter season.

#### 3.2 | Correlation of indexes with middle troposphere

Correlation analyses were performed to highlight centres of action represented by indexes, specifically to see similarities, differences and possible interactions among NCP, TDI\_MedT, TII\_EAT, EAWR, AO and NAO in different seasons (Figure 2).

The NCP and EAWR patterns had the highest agreement. The eastern pole of EAWR also appeared on NCP, and in fact, NCP had higher correlation scores at the Pacific coast, although it was calculated using data from the North Sea and the Caspian poles only. In contrast, TII\_EAT in winter (Figure 2j) was able to capture the east-west dipole within EM, despite being calculated using a single pole located at the west Pacific coast. Correlation patterns were remarkably similar in January for all indexes except for NAO (Figure 2). Centres of action belonging to the NCP or EAWR located over the North Sea and the Caspian were fairly stable throughout the year, but the pole at the Pacific coast moved westward in

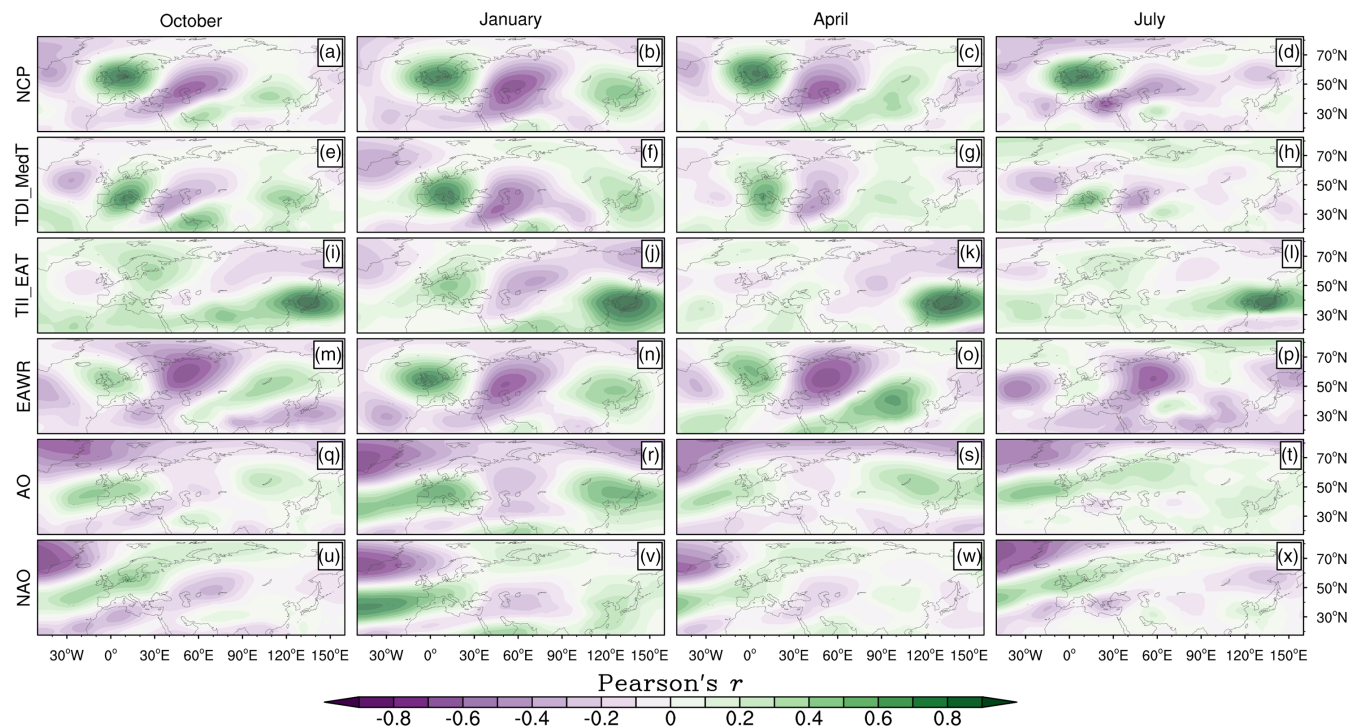


FIGURE 2 Correlation maps of indexes with  $z_{500}$  field for seasonal representative months [Colour figure can be viewed at [wileyonlinelibrary.com](http://wileyonlinelibrary.com)]

warmer seasons. When the poles of NCP and EAWR were compared, we observed that they are remarkably similar in terms of positioning, but the NCP was more sensitive to the pole located at the North Sea, and the Caspian pole of EAWR was positioned slightly northward. Loading patterns derived using PCA are expected to represent seasonal migration of “centre of actions,” because they are built to explain maximum variance (Hurrell & Deser, 2010). As we hardly saw any difference in the positioning of the poles of EAWR centred around the North Sea and the Caspian in different months of the year, it could be said that the NCP is very representative despite using fixed poles.

TII\_EAT and TDI\_MedT are only expected to be representative in winter since they utilize fixed poles to calculate seasonally varying centres of action. The NAO and AO patterns have a good fit between themselves specifically in the Atlantic sector where we see the north–south dipole clearly. That dipole pattern is prominent in winter, affects west of Europe, becomes less dominant in October and April, and is the weakest in July. While correlations associated with the AO are similar to the NAO over the Atlantic, the AO also has a good fit with other indexes in winter, specifically with TDI\_MedT and TII\_EAT over the EM. This similarity fades through the summer. These results suggest that the EAWR and NCP are in fact the same teleconnection, and NCP has a much broader extent than previously demonstrated.

### 3.3 | Composite differences

Composite differences of temperature and precipitation for the indexes being investigated are given in Figures 4 and 5, respectively. Only positive phases of indexes ( $z \geq 0.5$ ) are shown. Plots associated with the negative phases of temperature (Figure S5) and precipitation (Figure S6) composites are provided in the supporting material. Composites of  $z_{500}$  and  $z_{500}$  anomaly fields were overlaid to give a better insight about the working mechanism and hydroclimatological impacts of indexes (Figures 3 and S4).

Deviations in temperature indicated by NCP were attributed to 500 hPa anomaly circulations (Brunetti & Kutiel, 2011; Kutiel et al., 2002). We interpret this to be more of an advection of energy and moisture modification process. As the Mediterranean Trough is situated farther east the NCP, TDI\_MedT, TII\_EAT and EAWR indexes went into a positive phase, the Atlantic and adjacent regions experience more southwesterly flows leading to warmer temperatures, whereas Asia Minor and its surrounding regions experience more northwesterly flows resulting in cooler temperatures in the positive phase of the NCP (Figure 3). The Mediterranean Trough displacement index presents similar temperature anomaly patterns to those produced by the NCP(+); however, its dipole anomaly pattern is much closer to the Mediterranean, especially on the western side of the region.

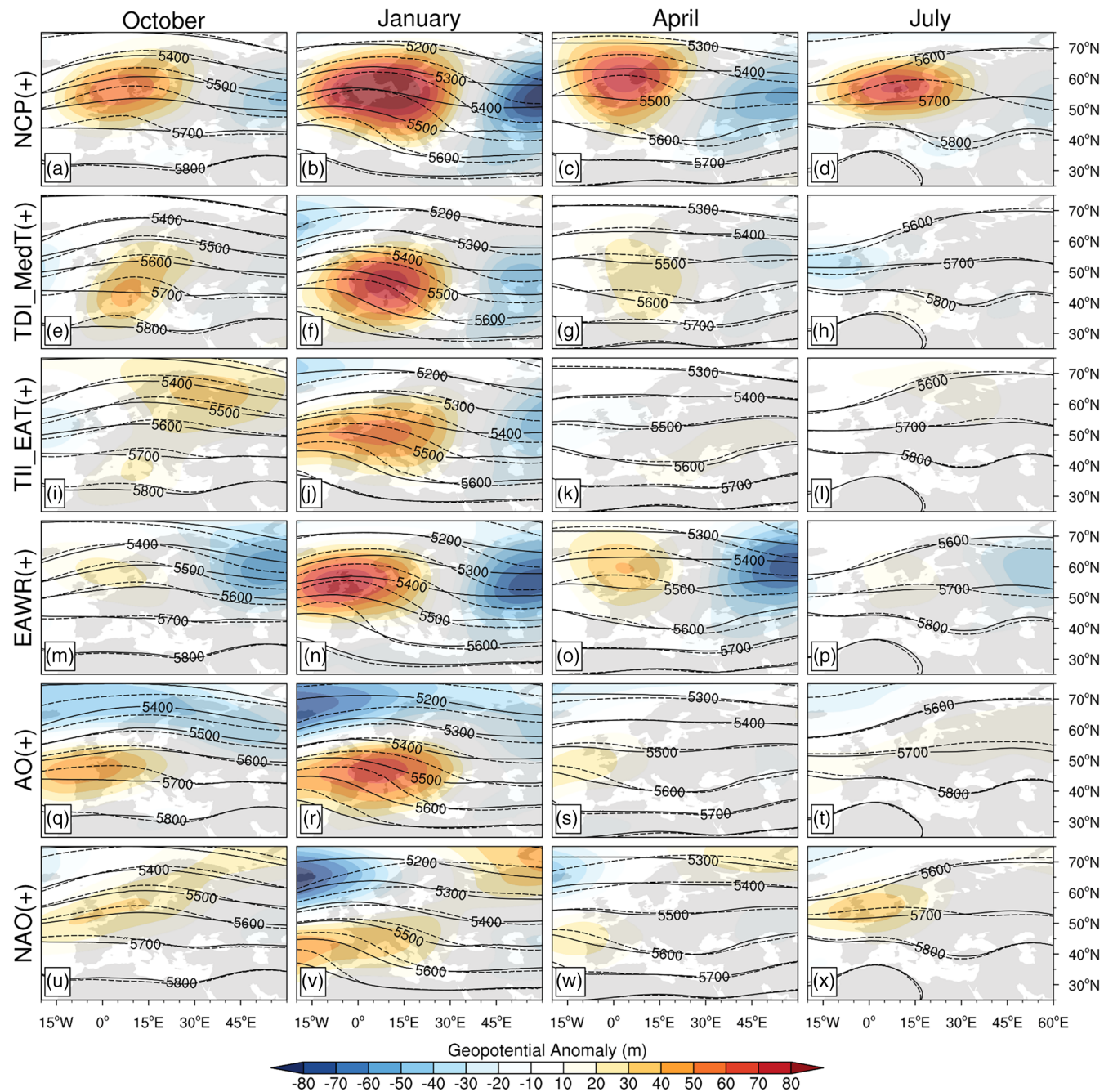


**FIGURE 3** Composite means of monthly mean 500 hPa thickness patterns corresponding to positive phases in the months of October, January, April and July. Continuous black lines indicate climatology and dashed lines indicate mean geopotential in the positive phase [Colour figure can be viewed at [wileyonlinelibrary.com](https://onlinelibrary.wiley.com/terms-and-conditions)]

Although being located far away and in the downstream of our domain, TII\_EAT was able to indicate an east-west dipole in the EM similar to the NCP, EAWR and AO in January (Figures 3j and S4j). The NCP composite anomalies show variations in strength but the patterns were similar in January, April, July and October. The contrast was at its peak in January, becoming slightly lower in July. These seasonal variations were visible in both temperature and precipitation composites.

The positive phase of TII\_EAT reveals similar but weaker temperature anomaly patterns to those of both NCP and TDI\_MedT, especially in October and January. It does not show, however, any significant influence on the EM climate variability in April and July. A very similar pattern to the NCP was observed on 500 hPa anomalies of the EAWR(+) but with higher contrast at the Caspian side, whereas the NCP(+) was more distinctive at the North Sea pole (Figure 3). Therefore, temperature

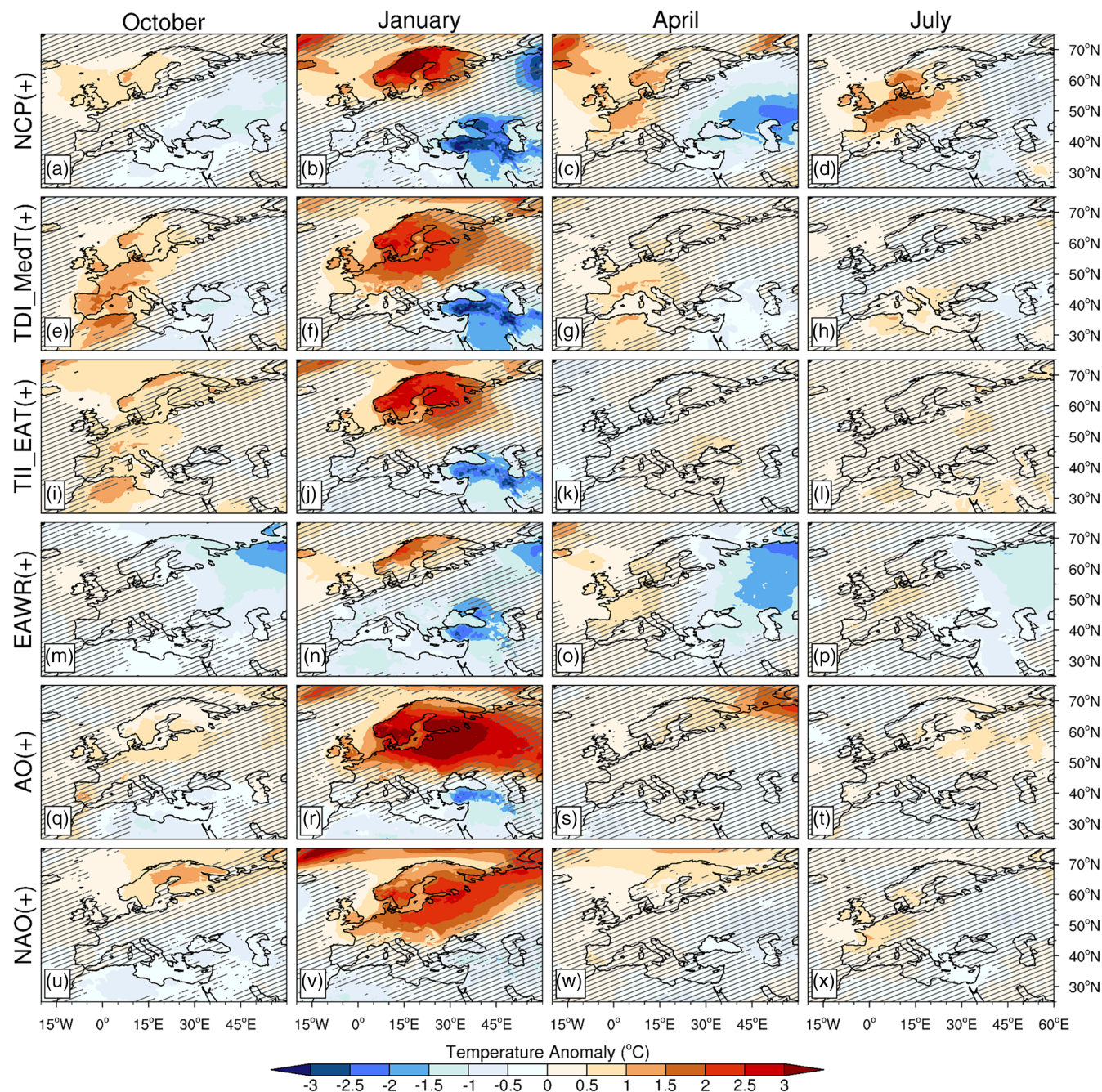


**FIGURE 4** Composite mean differences from monthly temperature climatology corresponding to positive phases in months October, January, April and July. Hatching shows areas where distributions of temperature involved with positive and negative phases are not significantly different according to the KS test [Colour figure can be viewed at [wileyonlinelibrary.com](https://onlinelibrary.wiley.com/terms-and-conditions)]

anomalies indicated by EAWR(+) were greater along the Ural-Siberian region compared to those of the NCP (Figure 4). The temperature variability depicted by the positive mode of AO resembles that of the NCP(+) in January, but the warming in northern Europe was more pronounced, while the cooling in Asia Minor was weaker than those of the NCP(+). The negative phase of the AO in winter was more similar to the NCP pattern than it was in the positive phase. In the negative phase, the

zonal contrast weakens and the meridional dipole over EM becomes more distinct. Compared to the AO(+) as well as the NCP(+) in January, the NAO(+) does not show a significant cooling anomaly across the Mediterranean side of the region, but it does produce a similar warming anomaly along with northern Europe. The textbook definition of the NAO impacts were only apparent in January. In the other months,  $z_{500}$ , precipitation, and temperature composites show smaller contrasts due to



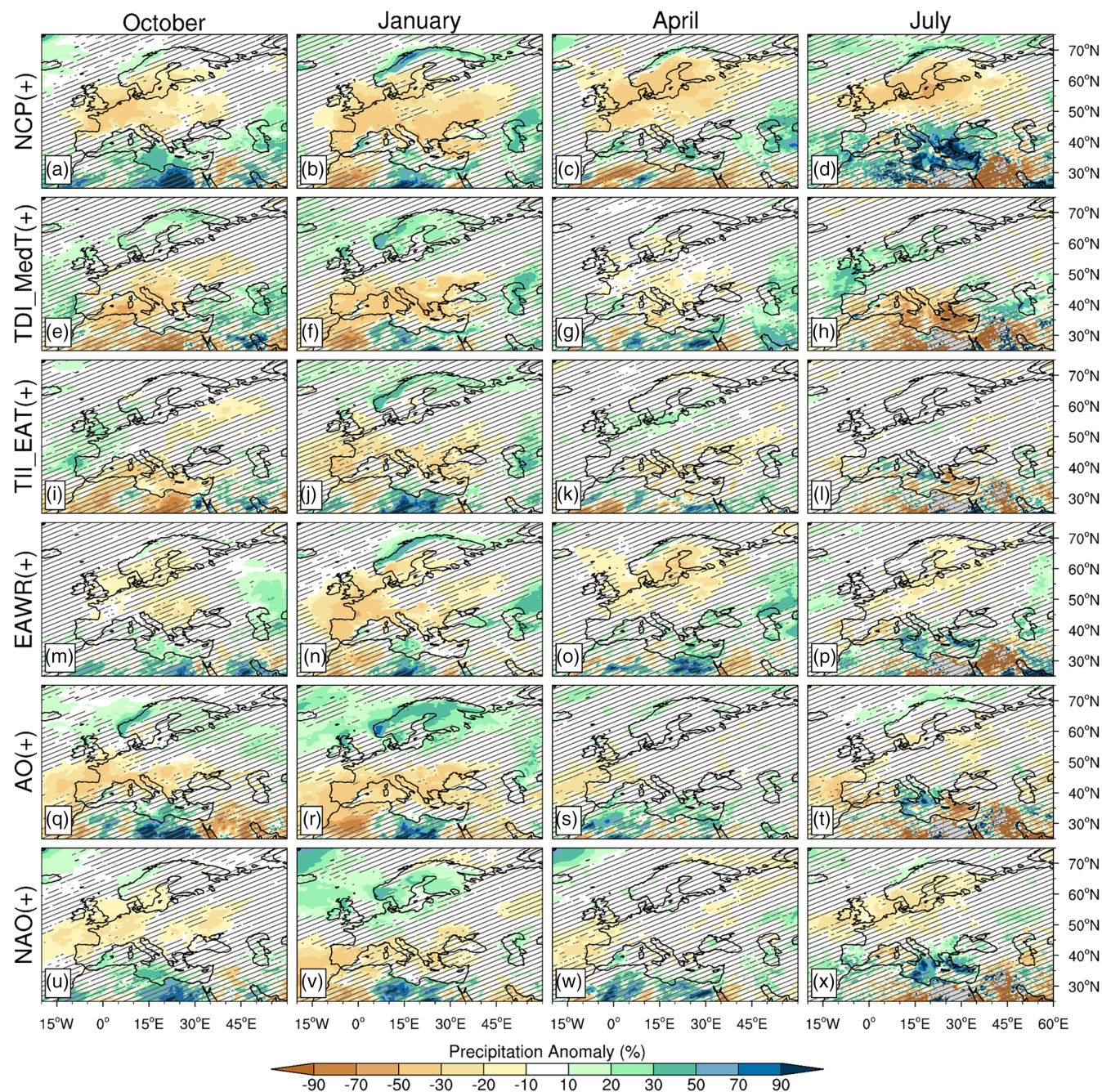


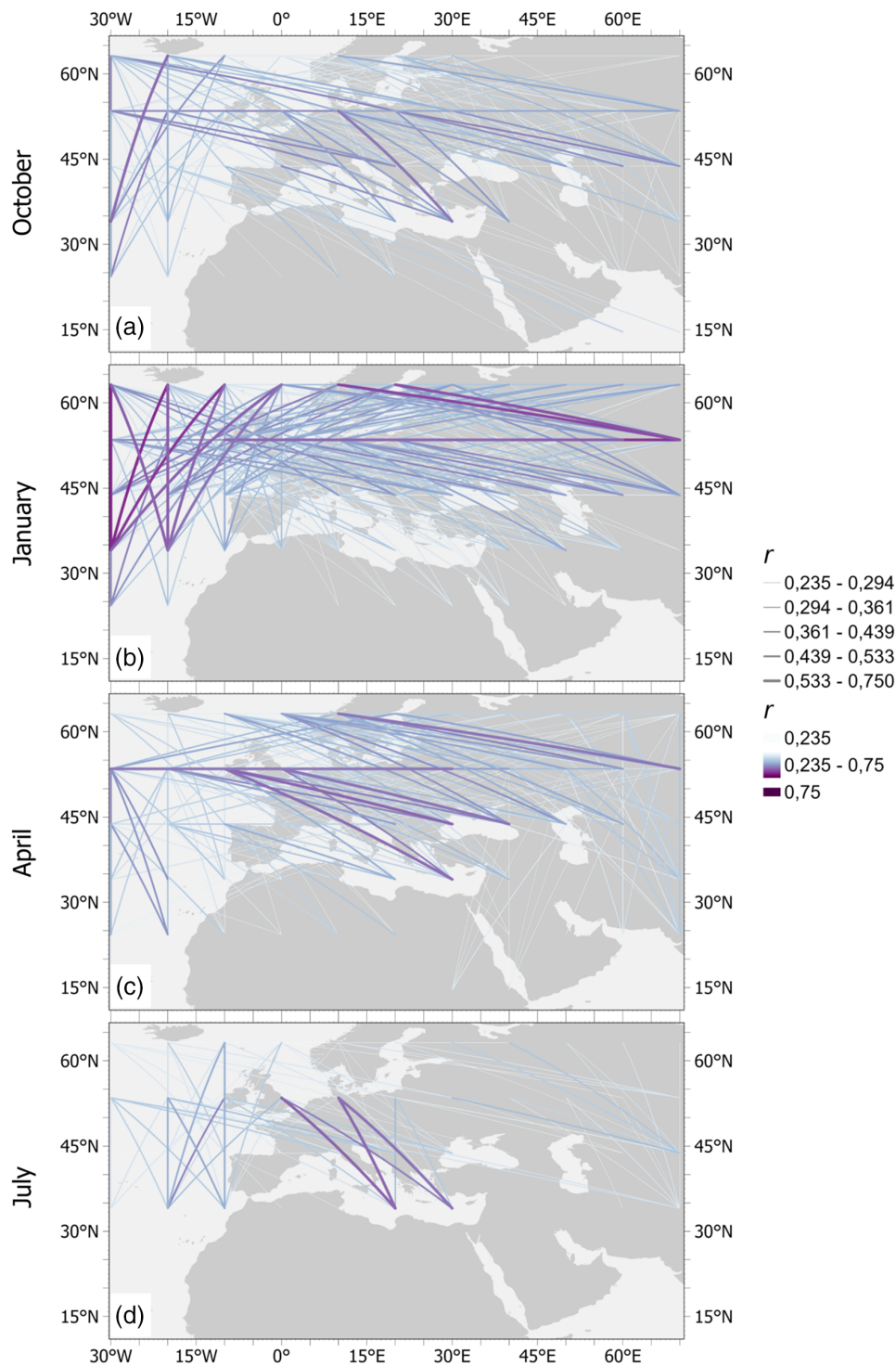
**FIGURE 5** Composite relative differences from monthly precipitation climatology corresponding to positive phases in months October, January, April and July. Hatching shows areas where distributions of precipitation involved with positive and negative phases are not significantly different according to the KS test [Colour figure can be viewed at [wileyonlinelibrary.com](https://onlinelibrary.wiley.com/terms-and-conditions)]

the NAO scores. The NCP, on the other hand, had spatially consistent anomaly patterns in the seasonally representative months of the year. Therefore, it could be said that the NCP is a competent teleconnection pattern that explains the hydroclimatological variability over the EM region in all seasons, seeming more robust than the others.

Brunetti and Kutiel (2011) asserted that the NCP had contradicting indications of precipitation anomalies in

different locations; therefore, it was not a suitable index for EM. Here, this was only true when we focused on a limited geographical extent. For instance, in Turkey, we see that the NCP(+) had opposite signals for precipitation in different months (Figure 5a–d). However, when we compared NCP to other indexes frequently examined, such as the EAWR pattern, AO and NAO, it was clear that NCP was better able to discriminate for precipitation in the EM. This result is consistent with the findings of

**FIGURE 6** Monthly maps of anti-correlations at  $z_{500}$  field for (a) October, (b) January, (c) April, (d) July as described in Kutiel and Benaroch (2002) where lines connect grid points with statistically significant negative correlations [Colour figure can be viewed at [wileyonlinelibrary.com](https://onlinelibrary.wiley.com/doi/10.1002/joc.8108)]



He et al. (2022), who showed that the NCP explains the drought pattern over the EM region better than the NAO. Here, negative precipitation anomalies indicated by the NCP(+) in Western and Central Europe moved northward from winter to summer. Northward retreating of centres of action from winter to summer were demonstrated via interannual standard deviations of monthly  $z_{500}$  fields (Figure S3), where higher deviations in  $z_{500}$  fields were expected to highlight centres of action.

Both NCP and EAWR presented similar contrasts demonstrated by composite anomalies, but due to being calculated by different methods, they presented some differences as well. Most obviously, NCP was more sensitive to deviations over the North Sea pole (Figures 2, 3 and S4). The North Sea was located at the upstream of the continent; therefore, limited moisture flux and suppressed cloud formation were significantly better represented due to high-pressure occurrences. As well as being

a hotspot for blocking events, the North Sea also experienced an increased number of those events specifically in April (Ionita et al., 2020). Apart from the complete formation of the wave train pattern, the NCP might be influenced by standalone blocking formations at the vicinity of North Sea since the pole-based method was less sensitive to the pattern, but more to the anomalies in the specified locations. Using RPCA and self-organizing maps (SOM) methods, Rousi et al. (2015) identified the kind of anomaly patterns which we suspect were signalling blocking events occurring over the North Sea. More to the point, the anticorrelation was not present between the North Sea and the Caspian Sea in summer (Figure 6d). July composites of  $z_{500}$  appeared more like a single anomaly centre over the North Sea rather than a dipole in the EM (Figures 3d and S4d). Similarly, Hatzaki et al. (2007) found that the NCP was not visible in summertime. However, precipitation anomalies (Figure 5a–d) indicated by the NCP were present in every month of the year (Çağlar et al., 2021; Müller-Plath et al., 2022). Here, the amplitude of geopotential height differences indicated by the NCP was larger in all months compared to the other indexes being inspected, and the spatial pattern of anomalies were more consistent in each month of the year (Figures 2, 3 and S4).

### 3.4 | Anticorrelation analysis

Anticorrelation analysis is another method to identify centres of action. By this analysis we reproduced the identification method of the NCP (Figure 6) used by Kutiel and Benaroch (2002). The period and re-analysis data in this study were different than in the original study, so sensitivity to these attributes were assessed. Although it was not mentioned in Kutiel and Benaroch's (2002) study, we think their anticorrelation figure was demonstrated for the month of December. We used a slightly different visualization technique, but we think both studies presented similar results (Figure S7). It was also demonstrated that centres of action are not stationary in terms of strength and positioning throughout the year. As mentioned earlier, the dipole pattern between the North Sea and the Caspian is not present in July, and strongest in January. Nonstationarity might not be limited to seasons but could also appear due to climate change. A study showed that there are interdecadal changes in positioning and magnitude of poles in loading patterns used for calculating PCs of the NAO in the last century (Vicente-Serrano & López-Moreno, 2008). It was shown that another dipole pattern, namely the Eastern Mediterranean Pattern (EMP), shifts towards northeast for  $\sim 10^\circ$  under a fossil

fuel developed future scenario for the end of the century (Hatzaki et al., 2009). Rousi et al. (2015) demonstrated that NCP as well as NAO in winter will be more prominent at the end of the century. Similarly, the Ural region is expected to experience more blocking events in future (He et al., 2017). The effect of climate change on NCP needs to be further investigated. Specifically, in order to identify possible effect of climate change triggered shifts in the positioning of centres of action, anticorrelation analysis should be repeated in higher resolution and for periods like recent past (1991–2020), distant past (1951–1980) and for periods in between. This is important because pole based calculated NCP is sensitive to positioning of centres.

The EM has been under the influence of various centres of action that control moisture advection into the continent (Batibeniz et al., 2020). Bozkurt et al. (2021) showed that a blocking system over the south of the Caspian Sea accompanied by the Mediterranean trough positioned over the Balkan region initiates atmospheric rivers which cause up to  $2 \text{ mm}\cdot\text{day}^{-1}$  precipitation anomalies in the headwaters section of Mesopotamia. The tails of these atmospheric rivers might extend as far as western tropical Africa. In these circumstances, it might be unrealistic to expect any teleconnection to successfully indicate rainfall anomalies in broad regions throughout the year. An earlier study (Sen et al., 2011), which was also related to the study of Bozkurt et al. (2021), was able to explain the anomalous snowmelt and precipitation events over the headwaters region of the Euphrates and Tigris basin through the changes in NCP. As shown in the same study, NAO did not show any signal to explain these anomalous events. Later, Sen et al. (2019) showed that these events are related to the position and amplitude of the Mediterranean trough. The present study demonstrated that NCP was also a good indicator of the Mediterranean trough positioning as there was a statistically significant relationship between NCP and TDI\_MedT.

## 4 | CONCLUSIONS

This study presents a comprehensive evaluation of the NCP, in comparison with other indexes, in explaining climate variability over the EM region using long-term high-resolution data of ERA5 reanalysis. The major contributions of the study are as follows:

- The NCP has relatively consistent spatial patterns throughout the year compared to other teleconnections being evaluated, although a small northerly shift from winter to summer is present. A northward retreat and

weakening of the Mediterranean Trough in summer explain contradicting signals of precipitation and temperature anomalies over Asia Minor and the Balkan Peninsula.

- The NCP is another representation of an EAWR teleconnection. The representation of the NCP is simpler than the RPCA-derived EAWR pattern, despite this, it explains variability better over the EM region.
- The NCP is useful for depicting not just temperature, but also precipitation anomalies in central, western, and northwestern parts of Europe.
- The NCP works on a much broader region than previously anticipated. In addition to the poles over the North Sea and the Caspian, it also has a third pole roughly at the north of China.
- Composite anomaly maps of temperature, precipitation, and  $z_{500}$  fields provide a high-resolution reference for the hydroclimatological impacts of key teleconnections in the EM.

It should be emphasized that the Mediterranean trough plays an important role in the climate variability of the Euro-Mediterranean region through its location, amplitude and strength. Further, the teleconnection patterns that are able to tackle these characteristics provide more information about the fluctuations in the climate of the region. Most of the teleconnection patterns seem to capture these features in the cold half of the year when the trough is also active over the southern parts of the region. When it retreats northwards and weakens, however, the teleconnections that only detect fluctuations in atmospheric fields over the Mediterranean latitudes fail to indicate climate deviations in the warm half of the year. The NCP, having one pole in the higher latitudes differs from these in that it is able to successfully detect warm season variability over the Euro-Mediterranean region as well. We used the name NCP since we followed the definition of calculation described in Kutiel et al. (2002), it addresses the centre of actions that are more persistent, and it has been well recognized. However, we think the early naming of the Eurasian was also appropriate for highlighting the broader geographic extent of the pattern.

#### AUTHOR CONTRIBUTIONS

**Ferat Çağlar:** Conceptualization; writing – review and editing; writing – original draft; methodology; visualization; data curation; formal analysis; software. **Omer Yetemen:** Conceptualization; writing – review and editing; funding acquisition; project administration; supervision. **Kwok Pan Chun:** Writing – review and editing; conceptualization; supervision. **Omer Lutfi Sen:** Writing – review and editing; conceptualization; supervision.

#### ACKNOWLEDGEMENTS

This study was supported by the 2232 International Fellowship for Outstanding Researchers Program of the Scientific and Technological Research Council of Turkey (TUBITAK) under grant 118C329. The financial support from TUBITAK does not mean that the content of the publication reflects the approved scientific view of TUBITAK. We thank Lucy Hyam for her kind help in proof-reading this paper for grammar and punctuation.

#### DATA AVAILABILITY STATEMENT

Surface fields and fields on pressure levels of ERA5 reanalysis data can be downloaded from <https://cds.climate.copernicus.eu/>. Time series of teleconnections are available through the NOAA CPC website <https://www.cpc.ncep.noaa.gov/data/teledoc/telecontents.shtml>.

#### ORCID

Ferat Çağlar  <https://orcid.org/0000-0002-2584-2883>

Omer Yetemen  <https://orcid.org/0000-0003-1593-3519>

Kwok Pan Chun  <https://orcid.org/0000-0001-9873-6240>

Omer Lutfi Sen  <https://orcid.org/0000-0002-8186-8594>

#### REFERENCES

- Ambaum, M.H.P., Hoskins, B.J. & Stephenson, D.B. (2001) Arctic Oscillation or North Atlantic Oscillation? *Journal of Climate*, 14(16), 3495–3507. Available from: [https://doi.org/10.1175/1520-0442\(2001\)014<3495:AONAO>2.0.CO;2](https://doi.org/10.1175/1520-0442(2001)014<3495:AONAO>2.0.CO;2)
- Ångström, A. (1935) Teleconnections of climatic changes in present time. *Geografiska Annaler*, 17(3–4), 242–258. Available from: <https://doi.org/10.1080/20014422.1935.11880600>
- Barnston, A.G. & Livezey, R.E. (1987) Classification, seasonality and persistence of low-frequency atmospheric circulation patterns. *Monthly Weather Review*, 115(6), 1083–1126. Available from: [https://doi.org/10.1175/1520-0493\(1987\)115<1083:CSAPOL>2.0.CO;2](https://doi.org/10.1175/1520-0493(1987)115<1083:CSAPOL>2.0.CO;2)
- Batibeniz, F., Ashfaq, M., Öno, B., Turuncoglu, U.U., Mehmood, S. & Evans, K.J. (2020) Identification of major moisture sources across the Mediterranean Basin. *Climate Dynamics*, 54(9–10), 4109–4127. Available from: <https://doi.org/10.1007/s00382-020-05224-3>
- Bell, B., Hersbach, H., Simmons, A., Berrisford, P., Dahlgren, P., Horányi, A. et al. (2021) The ERA5 global reanalysis: preliminary extension to 1950. *Quarterly Journal of the Royal Meteorological Society*, 147, 4186–4227. Available from: <https://doi.org/10.1002/qj.4174>
- Bozkurt, D., Sen, O.L., Ezber, Y., Guan, B., Viale, M. & Çağlar, F. (2021) Influence of African atmospheric Rivers on precipitation and snowmelt in the near East's highlands. *Journal of Geophysical Research: Atmospheres*, 126(4), e2020JD033646. Available from: <https://doi.org/10.1029/2020JD033646>
- Brunetti, M. & Kutiel, H. (2011) The relevance of the North-Sea Caspian pattern (NCP) in explaining temperature variability in Europe and the Mediterranean. *Natural Hazards and Earth System Science*, 11(10), 2881–2888. Available from: <https://doi.org/10.5194/nhess-11-2881-2011>

- Çağlar, F., Yetemen, O., Chun, K.P. & Sen, O.L. (2021) Applicability of the North Sea Caspian pattern as an indicator of the Euro-Mediterranean climate variability. *EGU General Assembly*, 2021, EGU21-8729. Available from: <https://doi.org/10.5194/egusphere-egu21-8729>
- Cheung, H.N., Zhou, W., Mok, H.Y. & Wu, M.C. (2012) Relationship between Ural-Siberian blocking and the East Asian winter monsoon in relation to the Arctic oscillation and the El Niño–Southern Oscillation. *Journal of Climate*, 25(12), 4242–4257. Available from: <https://doi.org/10.1175/JCLI-D-11-00225.1>
- Climate Prediction Center Internet Team. (2008) Teleconnection pattern calculation procedures. Available from: <https://www.cpc.ncep.noaa.gov/data/teledoc/telepatcalc.shtml>
- Conte, M., Giuffrida, A. & Tedesco, S. (1989) The Mediterranean oscillation: impact on precipitation and hydrology in Italy.
- Criado-Aldeanueva, F. & Soto-Navarro, F.J. (2013) The mediterranean oscillation teleconnection index: station-based versus principal component paradigms. *Advances in Meteorology*, 2013, 738501. Available from: <https://doi.org/10.1155/2013/738501>
- Criado-Aldeanueva, F. & Soto-Navarro, J. (2020) Climatic indices over the mediterranean sea: a review. *Applied Sciences (Switzerland)*, 10(17), 5790. Available from: <https://doi.org/10.3390/app10175790>
- Esbensen, S.K. (1984) A comparison of intermonthly and interannual teleconnections in the 700 mb geopotential height field during the Northern Hemisphere winter. *Monthly Weather Review*, 112(10), 2016–2032.
- Gao, T., Yu, J. & Paek, H. (2017) Impacts of four northern-hemisphere teleconnection patterns on atmospheric circulations over Eurasia and the Pacific. *Theoretical and Applied Climatology*, 129(3), 815–831. Available from: <https://doi.org/10.1007/s00704-016-1801-2>
- Ghasemi, A.R. & Khalili, D. (2008) The effect of the North Sea-Caspian pattern (NCP) on winter temperatures in Iran. *Theoretical and Applied Climatology*, 92(1), 59–74. Available from: <https://doi.org/10.1007/s00704-007-0309-1>
- Gündüz, M. & Özsoy, E. (2005) Effects of the North Sea Caspian pattern on surface fluxes of Euro-Asian-Mediterranean seas. *Geophysical Research Letters*, 32(21), 1–4. Available from: <https://doi.org/10.1029/2005GL024315>
- Hatzaki, M., Flocas, H.A., Asimakopoulos, D.N. & Maheras, P. (2007) The eastern Mediterranean teleconnection pattern: identification and definition. *International Journal of Climatology*, 27(6), 727–737. Available from: <https://doi.org/10.1002/joc.1429>
- Hatzaki, M., Flocas, H.A., Giannakopoulos, C. & Maheras, P. (2009) The impact of the eastern Mediterranean teleconnection pattern on the Mediterranean climate. *Journal of Climate*, 22(4), 977–992. Available from: <https://doi.org/10.1175/2008JCLI2519.1>
- He, Q., Xu, B., Dieppois, B., Yetemen, Ö., Sen, O.L., Klaus, J. et al. (2022) Impact of the North-Sea Caspian pattern on meteorological drought and vegetation response over diverging environmental systems in western Eurasia. *Ecohydrology*, 15, e2446. Available from: <https://doi.org/10.1002/eco.2446>
- He, S., Gao, Y., Li, F., Wang, H. & He, Y. (2017) Impact of Arctic oscillation on the East Asian climate: a review. *Earth-Science Reviews*, 164, 48–62. Available from: <https://doi.org/10.1016/j.earscirev.2016.10.014>
- Hersbach, H., Bell, B., Berrisford, P., Hirahara, S., Horányi, A., Muñoz-Sabater, J. et al. (2020) The ERA5 global reanalysis. *Quarterly Journal of the Royal Meteorological Society*, 146(730), 1999–2049. Available from: <https://doi.org/10.1002/qj.3803>
- Hurrell, J.W. (1995) Decadal trends in the North Atlantic Oscillation: regional temperatures and precipitation. *Science*, 269(5224), 676–679. Available from: <https://doi.org/10.1126/science.269.5224.676>
- Hurrell, J.W. & Deser, C. (2010) North Atlantic climate variability: the role of the North Atlantic Oscillation. *Journal of Marine Systems*, 79(3–4), 231–244. Available from: <https://doi.org/10.1016/j.jmarsys.2009.11.002>
- Hurrell, J.W., Kushnir, Y., Ottersen, G. & Visbeck, M. (2003) An overview of the North Atlantic oscillation. In: Hurrell, J.W., Kushnir, Y., Ottersen, G. & Visbeck, M. (Eds.) *The North Atlantic Oscillation: climatic significance and environmental impact*, Washington, DC: American Geophysical Union, pp. 1–35. Available from: <https://doi.org/10.1029/134GM01>
- Ionita, M. (2014) The impact of the East Atlantic/Western Russia pattern on the Hydroclimatology of Europe from mid-winter to late spring. *Climate*, 2(4), 296–309. Available from: <https://doi.org/10.3390/cli2040296>
- Ionita, M., Nagavciuc, V., Kumar, R. & Rakovec, O. (2020) On the curious case of the recent decade, mid-spring precipitation deficit in central Europe. *Npj Climate and Atmospheric Science*, 3(1), 1–10. Available from: <https://doi.org/10.1038/s41612-020-00153-8>
- Kalnay, E., Kanamitsu, M., Kistler, R., Collins, W., Deaven, D., Gandin, L. et al. (1996) The NCEP/NCAR 40-year reanalysis project. *Bulletin of the American Meteorological Society*, 77(3), 437–472. Available from: [https://doi.org/10.1175/1520-0477\(1996\)077<0437:TNYRP>2.0.CO;2](https://doi.org/10.1175/1520-0477(1996)077<0437:TNYRP>2.0.CO;2)
- Kistler, R., Kalnay, E., Collins, W., Saha, S., White, G., Woollen, J. et al. (2001) The NCEP–NCAR 50-year reanalysis: monthly means CD-ROM and documentation. *Bulletin of the American Meteorological Society*, 82(2), 247–268. Available from: [https://doi.org/10.1175/1520-0477\(2001\)082<0247:TNNYRM>2.3.CO;2](https://doi.org/10.1175/1520-0477(2001)082<0247:TNNYRM>2.3.CO;2)
- Krichak, S.O. & Alpert, P. (2005a) Decadal trends in the East Atlantic-West Russia pattern and Mediterranean precipitation. *International Journal of Climatology*, 25(2), 183–192. Available from: <https://doi.org/10.1002/joc.1124>
- Krichak, S.O. & Alpert, P. (2005b) Signatures of the NAO in the atmospheric circulation during wet winter months over the Mediterranean region. *Theoretical and Applied Climatology*, 82(1–2), 27–39. Available from: <https://doi.org/10.1007/s00704-004-0119-7>
- Krichak, S.O., Kishcha, P. & Alpert, P. (2002) Decadal trends of main Eurasian oscillations and the eastern Mediterranean precipitation. *Theoretical and Applied Climatology*, 72(3), 209–220. Available from: <https://doi.org/10.1007/s007040200021>
- Krown, L. (1966) An approach to forecasting seasonal rainfall in Israel. *Journal of Applied Meteorology*, 5(5), 590–594. Available from: [https://doi.org/10.1175/1520-0450\(1966\)005<0590:aatfsr>2.0.co;2](https://doi.org/10.1175/1520-0450(1966)005<0590:aatfsr>2.0.co;2)
- Kutiel, H. (2011) A review on the impact of the North Sea-Caspian pattern (NCP) on temperature and precipitation regimes in the Middle East. In: Gökçekus, H., Türker, U. & LaMoreaux, J.W. (Eds.) *Survival and sustainability: environmental concerns in the 21st century*. Berlin-Heidelberg: Springer, pp. 1301–1312. Available from: [https://doi.org/10.1007/978-3-540-95991-5\\_122](https://doi.org/10.1007/978-3-540-95991-5_122)

- Kutiel, H. & Benaroch, Y. (2002) North Sea-Caspian pattern (NCP)—an upper level atmospheric teleconnection affecting the Eastern Mediterranean: identification and definition. *Theoretical and Applied Climatology*, 71(1), 17–28. Available from: <https://doi.org/10.1007/s704-002-8205-x>
- Kutiel, H., Maheras, P., Türkeş, M. & Paz, S. (2002) North Sea-Caspian pattern (NCP)—an upper level atmospheric teleconnection affecting the eastern Mediterranean—implications on the regional climate. *Theoretical and Applied Climatology*, 72(3–4), 173–192. Available from: <https://doi.org/10.1007/s00704-002-0674-8>
- Kutiel, H. & Türkeş, M. (2005) New evidence for the role of the north sea—Caspian pattern on the temperature and precipitation regimes in continental central Turkey. *Geografiska Annaler: Series A, Physical Geography*, 87(4), 501–513. Available from: <https://doi.org/10.1111/j.0435-3676.2005.00274.x>
- Li, J., Yu, R. & Zhou, T. (2008) Teleconnection between NAO and climate downstream of the Tibetan Plateau. *Journal of Climate*, 21(18), 4680–4690. Available from: <https://doi.org/10.1175/2008JCLI2053.1>
- Lim, Y.K. (2015) The East Atlantic/West Russia (EA/WR) teleconnection in the North Atlantic: climate impact and relation to Rossby wave propagation. *Climate Dynamics*, 44(11–12), 3211–3222. Available from: <https://doi.org/10.1007/s00382-014-2381-4>
- Lionello, P., Bhend, J., Buzzi, A., Della-Marta, P.M., Krichak, S.O., Jansà, A. et al. (2006) Cyclones in the Mediterranean region: climatology and effects on the environment. In: Lionello, P., Malanotte-Rizzoli, P. & Boscolo, E.S. (Eds.) *Developments in earth and environmental sciences*, Vol. 4. Amsterdam: Elsevier, pp. 325–372. Available from: [https://doi.org/10.1016/S1571-9197\(06\)80009-1](https://doi.org/10.1016/S1571-9197(06)80009-1)
- Müller-Plath, G., Lüdecke, H.-J. & Lüning, S. (2022) Long-distance air pressure differences correlate with European rain. *Scientific Reports*, 12(1), 10191. Available from: <https://doi.org/10.1038/s41598-022-14028-w>
- Nigam, S. & Baxter, S. (2015) *General circulation of the atmosphere*. London: Academic Press, pp. 90–109. Available from: <https://doi.org/10.1016/B978-0-12-382225-3.00400-X>
- Panagiotopoulos, F., Shahgedanova, M. & Stephenson, D.B. (2002) A review of Northern Hemisphere winter-time teleconnection patterns. *Journal de Physique IV France*, 12(10), 27–47. Available from: <https://doi.org/10.1051/jp4:20020450>
- Rousi, E., Anagnostopoulou, C., Tolika, K. & Maheras, P. (2015) Representing teleconnection patterns over Europe: a comparison of SOM and PCA methods. *Atmospheric Research*, 152, 123–137. Available from: <https://doi.org/10.1016/j.atmosres.2013.11.010>
- Schloerke, B., Cook, D., Larmarange, J., Briatte, F., Marbach, M., Thoen, E. et al. (2021) GGally: extension to “ggplot2” (Version 2.1.0). Available from: <https://ggobi.github.io/ggally/>
- Schulzweida, U. (2022) CDO user guide. Zenodo. <https://doi.org/10.5281/zenodo.7112925>
- Sen, O.L., Ezber, Y. & Bozkurt, D. (2019) Euro-Mediterranean climate variability in boreal winter: a potential role of the East Asian trough. *Climate Dynamics*, 52(11), 7071–7084. Available from: <https://doi.org/10.1007/s00382-018-4573-9>
- Sen, O.L., Unal, A., Bozkurt, D. & Kindap, T. (2011) Temporal changes in the Euphrates and Tigris discharges and teleconnections. *Environmental Research Letters*, 6(2), 024012. Available from: <https://doi.org/10.1088/1748-9326/6/2/024012>
- Tatli, H. (2007) Synchronization between the North Sea–Caspian pattern (NCP) and surface air temperatures in NCEP. *International Journal of Climatology*, 27(9), 1171–1187. Available from: <https://doi.org/10.1002/joc.1465>
- The NCAR Command Language. (2019) *The NCAR Command Language software (Version 6.6.2)*. Boulder, CO: UCAR/NCAR-CISL/TDD. Available from: <https://doi.org/10.5065/D6WWD3XH5>
- Thompson, D.W.J.J. & Wallace, J.M. (1998) The Arctic oscillation signature in the wintertime geopotential height and temperature fields. *Geophysical Research Letters*, 25(9), 1297–1300. Available from: <https://doi.org/10.1029/98GL00950>
- Unal, Y.S., Deniz, A., Toros, H. & Incecik, S. (2012) Temporal and spatial patterns of precipitation variability for annual, wet, and dry seasons in Turkey. *International Journal of Climatology*, 32(3), 392–405. Available from: <https://doi.org/10.1002/joc.2274>
- Vicente-Serrano, S.M. & López-Moreno, J.I. (2008) Nonstationary influence of the North Atlantic Oscillation on European precipitation. *Journal of Geophysical Research: Atmospheres*, 113(20), 1–14. Available from: <https://doi.org/10.1029/2008JD010382>
- Wallace, J.M. & Gutzler, D.S. (1981) Teleconnections in the geopotential height field during the Northern Hemisphere winter. *Monthly Weather Review*, 109(4), 784–812. Available from: [https://doi.org/10.1175/1520-0493\(1981\)109<0784:TITGHF>2.0.CO;2](https://doi.org/10.1175/1520-0493(1981)109<0784:TITGHF>2.0.CO;2)
- Xoplaki, E., González-Rouco, J.F., Luterbacher, J. & Wanner, H. (2004) Wet season Mediterranean precipitation variability: influence of large-scale dynamics and trends. *Climate Dynamics*, 23(1), 63–78. Available from: <https://doi.org/10.1007/s00382-004-0422-0>
- Zhu, Z., Piao, S., Xu, Y., Bastos, A., Ciais, P. & Peng, S. (2017) The effects of teleconnections on carbon fluxes of global terrestrial ecosystems. *Geophysical Research Letters*, 44(7), 3209–3218. Available from: <https://doi.org/10.1002/2016GL071743>

## SUPPORTING INFORMATION

Additional supporting information can be found online in the Supporting Information section at the end of this article.

**How to cite this article:** Çağlar, F., Yetemen, O., Chun, K. P., & Sen, O. L. (2023). The merit of the North Sea-Caspian pattern in explaining climate variability in the Euro-Mediterranean region. *International Journal of Climatology*, 43(10), 4648–4661. <https://doi.org/10.1002/joc.8108>